

Pairing-induced speedup of nuclear spontaneous fission

Jhilam Sadhukhan,^{1,2,3,*} J. Dobaczewski,^{4,5,6} W. Nazarewicz,^{2,4,7} J. A. Sheikh,^{1,2} and A. Baran⁸

¹*Department of Physics and Astronomy, University of Tennessee, Knoxville, Tennessee 37996, USA*

²*Physics Division, Oak Ridge National Laboratory, P.O. Box 2008, Oak Ridge, Tennessee 37831, USA*

³*Physics Group, Variable Energy Cyclotron Centre, 1/AF Bidhan Nagar, Kolkata 700064, India*

⁴*Institute of Theoretical Physics, Faculty of Physics, University of Warsaw, Pasteura 5, PL-02-093 Warsaw, Poland*

⁵*Department of Physics, University of Jyväskylä, P.O. Box 35 (YFL), FI-40014 Jyväskylä, Finland*

⁶*Joint Institute of Nuclear Physics and Applications, P.O. Box 2008, Oak Ridge, Tennessee 37831, USA*

⁷*Department of Physics and Astronomy and NSCL/FRIB Laboratory, Michigan State University, East Lansing, Michigan 48824, USA*

⁸*Institute of Physics, University of M. Curie-Skłodowska, ul. Radziszewskiego 10, PL-20-031 Lublin, Poland*

(Received 4 October 2014; revised manuscript received 1 December 2014; published 22 December 2014)

Background: Collective inertia is strongly influenced at the level crossing at which the quantum system changes its microscopic configuration diabatically. Pairing correlations tend to make the large-amplitude nuclear collective motion more adiabatic by reducing the effect of these configuration changes. Competition between pairing and level crossing is thus expected to have a profound impact on spontaneous fission lifetimes.

Purpose: To elucidate the role of nucleonic pairing on spontaneous fission, we study the dynamic fission trajectories of ^{264}Fm and ^{240}Pu using the state-of-the-art self-consistent framework.

Methods: We employ the superfluid nuclear density functional theory with the Skyrme energy density functional SkM* and a density-dependent pairing interaction. Along with shape variables, proton and neutron pairing correlations are taken as collective coordinates. The collective inertia tensor is calculated within the nonperturbative cranking approximation. The fission paths are obtained by using the least action principle in a four-dimensional collective space of shape and pairing coordinates.

Results: Pairing correlations are enhanced along the minimum-action fission path. For the symmetric fission of ^{264}Fm , where the effect of triaxiality on the fission barrier is large, the geometry of the fission pathway in the space of the shape degrees of freedom is weakly impacted by pairing. This is not the case for ^{240}Pu , where pairing fluctuations restore the axial symmetry of the dynamic fission trajectory.

Conclusions: The minimum-action fission path is strongly impacted by nucleonic pairing. In some cases, the dynamical coupling between shape and pairing degrees of freedom can lead to a dramatic departure from the static picture. Consequently, in the dynamical description of nuclear fission, particle-particle correlations should be considered on the same footing as those associated with shape degrees of freedom.

DOI: [10.1103/PhysRevC.90.061304](https://doi.org/10.1103/PhysRevC.90.061304)

PACS number(s): 24.75.+i, 25.85.Ca, 21.60.Jz, 21.30.Fe

Introduction. Nuclear fission is a fundamental phenomenon that is a splendid example of a large-amplitude collective motion of a system in the presence of many-body tunneling. The corresponding equations involve potential, dissipative, and inertial terms [1]. The individual-particle motion gives rise to shell effects that influence the fission barriers and shapes on the way to fission and, also, strongly impact the inertia tensor through the crossings of single-particle levels and resulting configuration changes [2–4]. The residual interaction between crossing configurations is strongly affected by nucleonic pairing: the larger the pairing gap Δ , the more adiabatic is the collective motion [5–9].

The enhancement of pairing correlations along the fission path was postulated in Ref. [10] using simple physical arguments. Since the collective inertia roughly depends on the pairing gap as Δ^{-2} [5,11–14], by choosing a pathway with larger Δ , the fissioning nucleus can lower the collective action. This means that in searching for the minimum-action trajectory, the gap parameter should be treated as a dynamical variable. Indeed, macroscopic-microscopic studies [15–18]

have demonstrated that pairing fluctuations can significantly reduce the collective action and, hence, affect the predicted spontaneous fission (SF) lifetimes.

Our long-term goal is to describe SF within the superfluid nuclear density functional theory by minimizing the collective action in many-dimensional collective space. The important milestone was a recent paper [19] which demonstrated that predicted SF pathways strongly depend on the choice of the collective inertia and approximations involved in treating level crossings. The main objective of the present work is to elucidate the role of nucleonic pairing in SF by studying the dynamic fission trajectories of ^{264}Fm and ^{240}Pu in a four-dimensional collective space. In addition to two quadrupole moments defining the elongation and triaxiality of nuclear shape we consider the strengths of neutron and proton pairing fluctuations. Since in our model the effect of triaxiality on the fission barrier is larger for ^{264}Fm (~ 4 MeV) [20] than for ^{240}Pu (~ 2 MeV) [21], by considering these two cases we can study the interplay between pairing dynamics and symmetry-breaking effects [8,22].

Theoretical framework. To calculate the SF half-life, we closely follow the formalism described in Ref. [19]. In the semiclassical approximation, the SF half-life can be written

*jhilam@vecc.gov.in

as [23,24] $T_{1/2} = \ln 2 / (nP)$, where n is the number of assaults on the fission barrier per unit time (here we adopt the standard value of $n = 10^{20.38} \text{ s}^{-1}$) and $P = 1/(1 + e^{2S})$ is the penetration probability expressed in terms of the fission action integral,

$$S(L) = \int_{s_{\text{in}}}^{s_{\text{out}}} \frac{1}{\hbar} \sqrt{2\mathcal{M}_{\text{eff}}(s)(V(s) - E_0)} ds, \quad (1)$$

calculated along the fission path $L(s)$. The effective inertia $\mathcal{M}_{\text{eff}}(s)$ [19,23–25] is obtained from the multidimensional nonperturbative cranking inertia tensor \mathcal{M}^C . E_0 is the collective ground-state energy, and ds is the element of length along $L(s)$. To compute the potential energy V , we subtract the vibrational zero-point energy E_{ZPE} from the Hartree-Fock-Bogoliubov (HFB) energy E_{HFB} obtained self-consistently from the constrained HFB equations for the Routhian,

$$\hat{H}' = \hat{H}_{\text{HFB}} - \sum_{\mu=0,2} \lambda_{\mu} \hat{Q}_{2\mu} - \sum_{\tau=n,p} (\lambda_{\tau} \hat{N}_{\tau} - \lambda_{2\tau} \Delta \hat{N}_{\tau}^2), \quad (2)$$

where \hat{H}_{HFB} , $\hat{Q}_{2\mu}$, and \hat{N}_{τ} represent the HFB Hamiltonian, axial ($\mu = 0$) and nonaxial ($\mu = 2$) components of the mass quadrupole moment operator, and neutron ($\tau = n$) and proton ($\tau = p$) particle-number operators, respectively. The particle-number dispersion terms $\Delta \hat{N}_{\tau}^2 = \hat{N}_{\tau}^2 - \langle \hat{N}_{\tau} \rangle^2$, controlled by the Lagrange multipliers $\lambda_{2\tau}$, determine the dynamic pairing correlations of the system [26,27]. That is, $\lambda_{2\tau} = 0$ corresponds to the static HFB pairing. Dynamic pairing fluctuations stronger than those obtained within the static solution are described by $\lambda_{2\tau} > 0$. The overall magnitude of pairing correlations (static + dynamic) can be related to the average pairing gap Δ_{τ} [28,29]. In this study, $\lambda_{2\tau}$ are used as two independent dynamical coordinates to scan over a wide range of pairing correlations (or Δ_{τ}).

The one-dimensional path $L(s)$ is defined in the multidimensional collective space by specifying the collective variables $\{X_i\} \equiv \{Q_{20}, Q_{22}, \lambda_{2n} + \lambda_{2p}, \lambda_{2n} - \lambda_{2p}\}$ as functions of the path's length s . Furthermore, to render collective coordinates dimensionless, we define $x_i = X_i / \delta x_i$, where δx_i are appropriate scale parameters that are also used when determining numerical derivatives of density matrices [30]. Although the collective action is invariant to uniform scaling, working with dimensionless ds is simply convenient when defining the fission path and analyzing results. We take $\delta x_1 = \delta x_2 = 1$ b [30], whereas values of $\delta x_3 = \delta x_4 = 0.01$ MeV were selected after numerical tests of the corresponding derivatives. Namely, we checked that the inertia tensor does not change by increasing these steps up to a value as large as 0.05 MeV. The dynamical coordinates x_3 and x_4 control, respectively, the isoscalar and isovector pairing fluctuations.

As a continuation of our previous study [19], we first consider the SF of ^{264}Fm , which is predicted to undergo a symmetric split into two doubly magic ^{132}Sn fragments [31]. Therefore, the crucial shape degrees of freedom in this case are elongation and triaxiality; they are represented by quadrupole moments Q_{20} and Q_{22} defined as in Table 5 in Ref. [32]. To compute the total energy E_{HFB} and inertia tensor \mathcal{M}^C , we employ the symmetry-unrestricted HFB solver HFODD

(v2.49t) [33]. To be consistent with the previous work [19], we use the Skyrme energy density functional SkM* [34] in the particle-hole channel.

The particle-particle interaction is approximated by the density-dependent mixed pairing force [35]. The E_{ZPE} is estimated by using the Gaussian overlap approximation [16,36,37]. To obtain the expression for E_{ZPE} , we neglected the derivatives of the pairing fields with respect to $\lambda_{2\tau}$, as we found that the variation of the average pairing gap with $\lambda_{2\tau}$ is quite small. Moreover, we checked that the topology of the fission path is barely sensitive to the detailed structure of the E_{ZPE} .

The inertia tensor \mathcal{M}^C was obtained from the nonperturbative cranking approximation to the adiabatic time-dependent HFB as described in Refs. [19] and [30]. The density-matrix derivatives with respect to the collective coordinates used to compute \mathcal{M}^C [30] were obtained by using finite differences with steps δq_i . Finally, to obtain the minimum-action pathways we adopted two independent algorithms to ensure the robustness of the result: the dynamical programming method [23] and the Ritz method [24]. In all cases considered, both approaches give consistent answers.

Results. In the first step, to assess the relative importance of isoscalar and isovector pairing degrees of freedom, the minimum-action path was calculated in the three-dimensional (3D) space of coordinates x_1 , x_3 , and x_4 . To this end, we adopted a $90 \times 61 \times 31$ mesh with $21 \leq x_1 \leq 110$, $-10 \leq x_3 \leq 50$, and $-15 \leq x_4 \leq 15$. Coordinate x_2 was fixed according to the two-dimensional (2D) dynamical path in Ref. [19]. The contour maps of V in the x_1 - x_3 plane for $x_4 = 0$ and the x_1 - x_4 plane for $x_3 = 0$ are displayed in Fig. 1 (left).

Since the individual components of the full (3D) inertia tensor are difficult to interpret, following [19] in Fig. 1 (right) we show the cubic root determinant of the inertia tensor

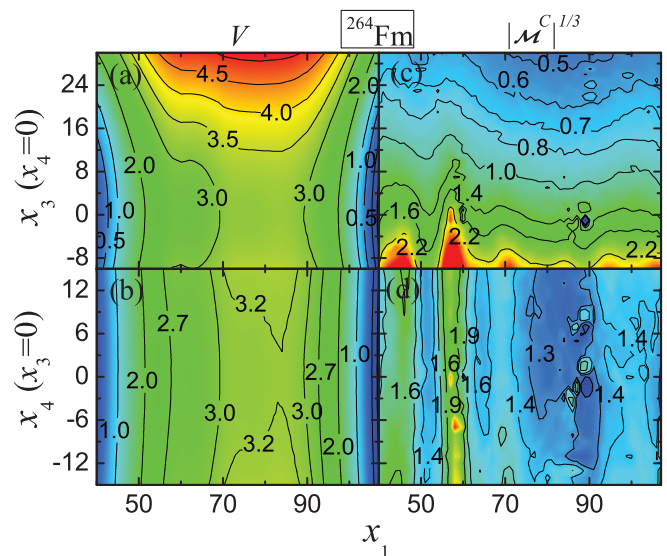


FIG. 1. (Color online) Contour maps of V (left; in MeV) and $|\mathcal{M}^C|^{1/3}$ (right; in $\hbar^2 \text{ MeV}^{-1}/1000$), calculated for ^{264}Fm in the x_1 - x_3 plane for $x_4 = 0$ (top) and the x_1 - x_4 plane for $x_3 = 0$ (bottom). Energies are plotted relatively to the ground-state value.

$|\mathcal{M}_C|^{1/3}$. It can be seen that at large values of x_3 , the peaks in $|\mathcal{M}^C|^{1/3}$ due to level crossings disappear, and moreover, the magnitude of inertia generally decreases with x_3 . This is consistent with general expectations for the effect of pairing on the collective inertia. On the other hand, variations in x_4 have little effect on $|\mathcal{M}^C|^{1/3}$ and V . This result is confirmed by computing the minimum-action path in the (x_1, x_3, x_4) space: the fissioning system prefers to maintain large proton and neutron pairing gaps and, at the same time, $x_4 \approx 0$. Consequently, in the SF, this degree of freedom seems to play a less important role.

In previous work, we have shown that the minimum-action path breaks the axial symmetry to avoid level crossings and minimize the level density of single-particle states around the Fermi level. In contrast, pairing correlations grow with the single-particle level density. Consequently, pairing is expected to impact V and \mathcal{M}_{eff} in a different way. Namely, as pairing (or x_3) increases, the potential energy is expected to grow—as one departs from the self-consistent value—while the collective inertia is reduced. The interplay between these two opposing tendencies determines the minimum-action trajectory. To evaluate how the fission path is modified due to pairing, in the next step we minimize the collective action in the (x_1, x_2, x_3) space. Here we assume $x_4 = 0$ and adopt the value of $E_0 = 1$ MeV to be consistent with Ref. [19]. Figure 2 displays the resulting contour maps of V and $|\mathcal{M}^C|^{1/3}$. The upper panels correspond to the situation discussed in Ref. [19], in which dynamical pairing is disregarded ($x_3 = 0$). As shown in Fig. 2(a), the triaxial coordinate x_2 reduces the fission barrier height by slightly more than 4 MeV. The fluctuations in $|\mathcal{M}^C|^{1/3}$ shown in Fig. 2(c) reflect crossings of single-particle levels at the Fermi level. The results shown in the lower panels correspond to the axial shape ($x_2 = 0$); they are again consistent with the general dependence of the potential energy and collective inertia on the pairing correlations.

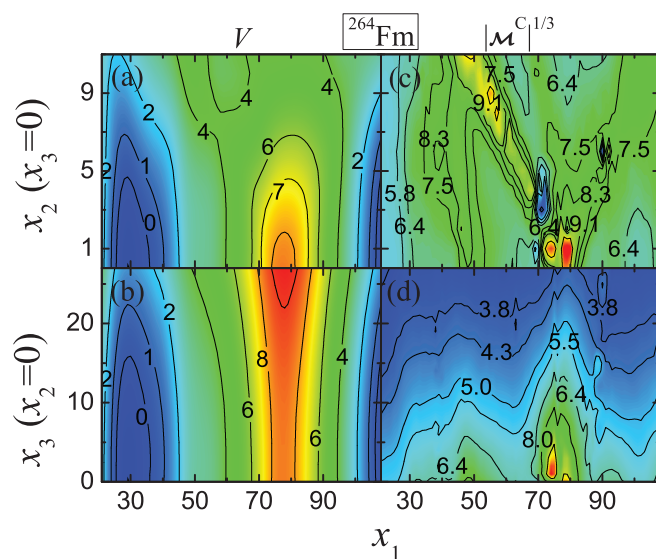


FIG. 2. (Color online) Similar to Fig. 1 except for the x_1 - x_2 plane for $x_3 = x_4 = 0$ (top) and the x_1 - x_3 plane for $x_2 = x_4 = 0$ (bottom).

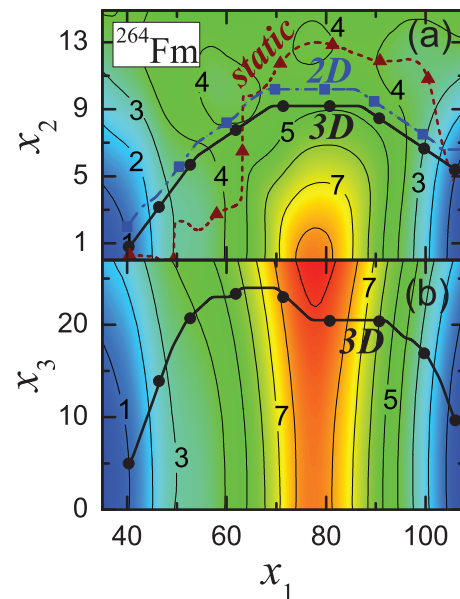


FIG. 3. (Color online) Projections of the three-dimensional (3D; solid line) dynamic SF path for ^{264}Fm (a) on the x_1 - x_2 plane for $x_3 = x_4 = 0$ and (b) on the x_1 - x_3 plane for $x_2 = x_4 = 0$, calculated using the dynamical programming method technique. The dash-dotted line shows, for comparison, the two-dimensional (2D) path computed without pairing fluctuations. The static SF path corresponding to the minimized collective potential [19] is also plotted (dotted line). Symbols on the paths denote the path lengths in units of 10. Potentials V of Fig. 2 are drawn as a background reference.

In Figs. 3(a) and 3(b), we show projections of the minimum-action path onto the x_1 - x_2 and x_1 - x_3 planes, respectively. The 2D fission path calculated without pairing fluctuations ($x_3 = x_4 = 0$) and the static SF path corresponding to the valley of the minimized collective potential are also shown for comparison. Evidently, the triaxiality along the 3D fission path is reduced at the expense of enhanced pairing. Nevertheless, owing to the reduced action of S , the calculated SF half-life of ^{264}Fm in the 3D variant is decreased by as much as three decades.

Figure 4 summarizes our results for ^{264}Fm . Namely, it shows V , $\mathcal{M}_{\text{eff}}^C$, S , and Δ_τ along the fission paths calculated with dynamical (3D) and static (2D) pairing. Compared to the 2D path, the 3D path is shorter and it favors a lower collective inertia at the cost of a higher potential energy, both being the result of enhanced pairing correlations. It is interesting to note that the collective potentials V in two dimensions and three dimensions are fairly different, and they both deviate from the static result, which is usually interpreted in terms of a fission barrier or a saddle point.

While the minimum-action pathways in ^{264}Fm are not that far from the static SF path, this is not the case for ^{240}Pu , where the energy gain on the first barrier resulting from triaxiality is around 2 MeV, that is, significantly less than in ^{264}Fm . To illustrate the impact of pairing fluctuations on the SF of ^{240}Pu , we consider the minimum-action collective path between its ground state and the superdeformed fission isomer. In this region of collective space, reflection-asymmetric degrees of

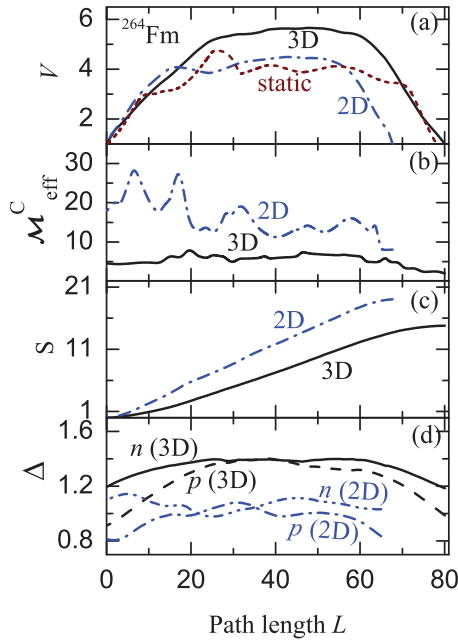


FIG. 4. (Color online) (a) Potential V (in MeV), (b) effective inertia $\mathcal{M}_{\text{eff}}^C$ (in $\hbar^2 \text{MeV}^{-1}/1000$), (c) action S , and (d) average pairing gaps Δ_n and Δ_p (in MeV) plotted along the 2D (static pairing; dotted line) and 3D (dynamic pairing; solid line) paths. The static fission barrier is displayed for comparison in (a).

freedom are less important; hence, the 3D space of (x_1, x_2, x_3) is adequate.

As shown in Fig. 5, in the region of the first saddle in the static calculations, the impact of dynamics on the minimum-action pathway for ^{240}Pu is dramatic. Compared to

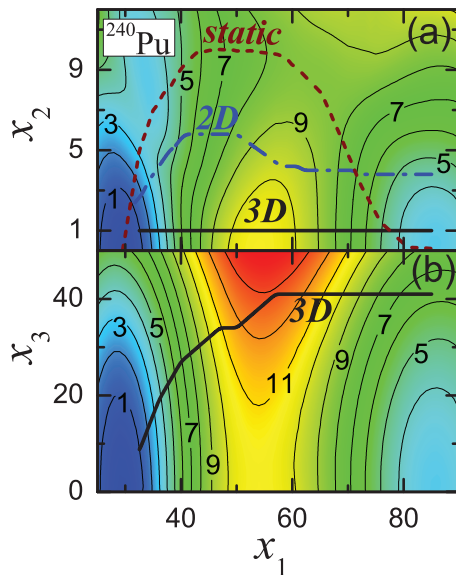


FIG. 5. (Color online) Similar to Fig. 3 but for ^{240}Pu . The static SF path is represented by the dotted line.

the static-pairing calculation, in the 2D calculations the effect of triaxiality is significantly reduced, and in 3D calculations the axial symmetry of the system is fully restored.

Conclusions. In this study, we have extended the self-consistent minimum-action approach to the SF by considering collective coordinates associated with pairing. Our approach takes into account essential ingredients impacting the SF dynamics [22]: (i) spontaneous breaking of mean-field symmetries; (ii) diabatic configuration changes due to level crossings; (iii) reduction of nuclear inertia by pairing; and (iv) dynamical fluctuations governed by the minimum-action principle.

We have demonstrated that the SF pathways and lifetimes are significantly influenced by the nonperturbative collective inertia and dynamical fluctuations in shape and pairing degrees of freedom. While the reduction of the collective action by pairing fluctuations has been pointed out in earlier works [10, 13, 15–17] and also very recently in a self-consistent approach [38], our work shows that pairing dynamics can profoundly impact the penetration probability, that is, effective fission barriers, by restoring symmetries spontaneously broken in a static approach.

Our calculations for ^{264}Fm and ^{240}Pu show that the dynamical coupling between shape and pairing degrees of freedom can lead to a dramatic departure from the standard static picture based on saddle points obtained in static mean-field calculations. In particular, for ^{240}Pu , pairing fluctuations restore the axial symmetry around the fission barrier, which, in the static approach, is broken spontaneously. The examples presented in this work, in particular, in Figs. 4 and 5, illustrate how limited the notion of fission barrier is.

Future improvements, aiming at systematic comparison with experiment, will include the full adiabatic time-dependent HFB treatment of collective inertia, addition of reflection asymmetric collective coordinates, and use of energy density functionals optimized for fission [39]. Work along all these lines is in progress.

Acknowledgments. Discussions with G. F. Bertsch, K. Mazurek, and N. Schunck are gratefully acknowledged. This study was initiated during Program INT-13-3, “Quantitative Large Amplitude Shape Dynamics: Fission and Heavy Ion Fusion,” at the National Institute for Nuclear Theory in Seattle, Washington. This material is based on work supported by the U.S. Department of Energy, Office of Science, Office of Nuclear Physics, under Award No. DE-FG02-96ER40963 (University of Tennessee) and No. DE-SC0008499 (NUCLEI SciDAC Collaboration); by the NNSA’s Stewardship Science Academic Alliances Program under Award No. DE-FG52-09NA29461 (the Stewardship Science Academic Alliances program); by the Academy of Finland and University of Jyväskylä within the FIDIPRO program; and by the Polish National Science Center under Contract No. 2012/07/B/ST2/03907. An award of computer time was provided by the National Institute for Computational Sciences (NICS) and the Innovative and Novel Computational Impact on Theory and Experiment (INCITE) program using resources of the OLCF facility.

- [1] W. Swiatecki and S. Bjørnholm, *Phys. Rep.* **4**, 325 (1972).
- [2] D. L. Hill and J. A. Wheeler, *Phys. Rev.* **89**, 1102 (1953).
- [3] L. Wilets, *Phys. Rev.* **116**, 372 (1959).
- [4] R. W. Hasse, *Rep. Prog. Phys.* **41**, 1027 (1978).
- [5] M. Brack, J. Damgaard, A. S. Jensen, H. C. Pauli, V. M. Strutinsky, and C. Y. Wong, *Rev. Mod. Phys.* **44**, 320 (1972).
- [6] G. Schütte and L. Wilets, *Nucl. Phys. A* **252**, 21 (1975); *Z. Phys. A* **286**, 313 (1978).
- [7] V. Strutinsky, *Z. Phys. A* **280**, 99 (1977).
- [8] W. Nazarewicz, *Nucl. Phys. A* **557**, 489 (1993).
- [9] T. Nakatsukasa and N. R. Walet, *Phys. Rev. C* **57**, 1192 (1998).
- [10] L. G. Moretto and R. P. Babinet, *Phys. Lett. B* **49**, 147 (1974).
- [11] M. Urin and D. Zaretsky, *Nucl. Phys.* **75**, 101 (1966).
- [12] T. Ledergerber and H.-C. Pauli, *Nucl. Phys. A* **207**, 1 (1973).
- [13] Y. A. Lazarev, *Phys. Scripta* **35**, 255 (1987).
- [14] K. Pomorski, *Int. J. Mod. Phys. E* **16**, 237 (2007).
- [15] A. Staszczak, A. Baran, K. Pomorski, and K. Böning, *Phys. Lett. B* **161**, 227 (1985).
- [16] A. Staszczak, S. Piłat, and K. Pomorski, *Nucl. Phys. A* **504**, 589 (1989).
- [17] Z. Łojewski and A. Staszczak, *Nucl. Phys. A* **657**, 134 (1999).
- [18] M. Mirea and R. C. Bobulescu, *J. Phys. G* **37**, 055106 (2010).
- [19] J. Sadhukhan, K. Mazurek, A. Baran, J. Dobaczewski, W. Nazarewicz, and J. A. Sheikh, *Phys. Rev. C* **88**, 064314 (2013).
- [20] A. Staszczak, A. Baran, and W. Nazarewicz, *Int. J. Mod. Phys. E* **20**, 552 (2011).
- [21] J. A. Sheikh, W. Nazarewicz, and J. C. Pei, *Phys. Rev. C* **80**, 011302 (2009).
- [22] J. Negele, *Nucl. Phys. A* **502**, 371 (1989).
- [23] A. Baran, K. Pomorski, A. Lukasiak, and A. Sobczewski, *Nucl. Phys. A* **361**, 83 (1981).
- [24] A. Baran, *Phys. Lett. B* **76**, 8 (1978).
- [25] A. Baran, Z. Łojewski, K. Sieja, and M. Kowal, *Phys. Rev. C* **72**, 044310 (2005).
- [26] N. L. Vaquero, T. R. Rodríguez, and J. L. Egido, *Phys. Lett. B* **704**, 520 (2011).
- [27] N. L. Vaquero, J. L. Egido, and T. R. Rodríguez, *Phys. Rev. C* **88**, 064311 (2013).
- [28] J. Dobaczewski, H. Flocard, and J. Treiner, *Nucl. Phys. A* **422**, 103 (1984).
- [29] J. Dobaczewski, W. Nazarewicz, and T. R. Werner, *Phys. Scripta* **1995**, 15 (1995).
- [30] A. Baran, J. A. Sheikh, J. Dobaczewski, W. Nazarewicz, and A. Staszczak, *Phys. Rev. C* **84**, 054321 (2011).
- [31] A. Staszczak, A. Baran, J. Dobaczewski, and W. Nazarewicz, *Phys. Rev. C* **80**, 014309 (2009).
- [32] J. Dobaczewski and P. Olbratowski, *Comput. Phys. Commun.* **158**, 158 (2004).
- [33] N. Schunck, J. Dobaczewski, J. McDonnell, W. Satuła, J. Sheikh, A. Staszczak, M. Stoitsov, and P. Toivanen, *Comput. Phys. Commun.* **183**, 166 (2012).
- [34] J. Bartel, P. Quentin, M. Brack, C. Guet, and H.-B. Håkansson, *Nucl. Phys. A* **386**, 79 (1982).
- [35] J. Dobaczewski, W. Nazarewicz, and M. Stoitsov, *Eur. Phys. J. A* **15**, 21 (2002).
- [36] A. Baran, A. Staszczak, J. Dobaczewski, and W. Nazarewicz, *Int. J. Mod. Phys. E* **16**, 443 (2007).
- [37] A. Staszczak, A. Baran, and W. Nazarewicz, *Phys. Rev. C* **87**, 024320 (2013).
- [38] S. A. Giuliani, L. M. Robledo, and R. Rodríguez-Guzmán, *Phys. Rev. C* **90**, 054311 (2014).
- [39] M. Kortelainen, J. McDonnell, W. Nazarewicz, P.-G. Reinhard, J. Sarich, N. Schunck, M. V. Stoitsov, and S. M. Wild, *Phys. Rev. C* **85**, 024304 (2012).